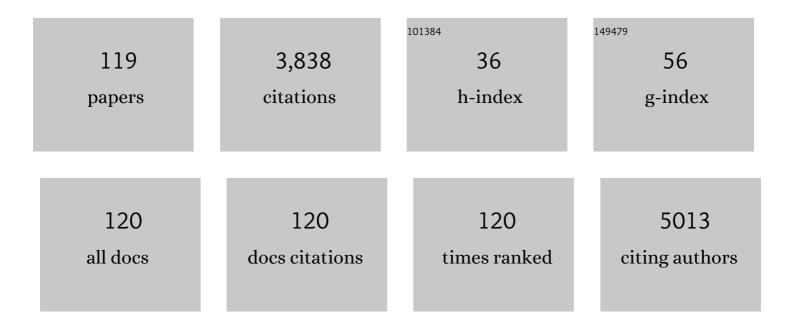
## Chinnuswamy Viswanathan

List of Publications by Year in descending order

Source: https://exaly.com/author-pdf/8291455/publications.pdf Version: 2024-02-01



#	Article	IF	CITATIONS
1	SnO2 nanoflakes deposited carbon yarn-based electrochemical immunosensor towards cortisol measurement. Journal of Nanostructure in Chemistry, 2023, 13, 115-127.	5.3	12
2	Waste cigarette butt derived Carbon/Magnesium oxide nanocomposite as potential adsorbent for the removal of ciprofloxacin from waste water. Materials Letters, 2022, 312, 131668.	1.3	4
3	Engineering the semiconducting CdS nanostructures by N-doped rGO for enhancing the adsorption sites: Promising electrocatalyst for hydrogen evolution reaction. International Journal of Hydrogen Energy, 2022, 47, 16106-16120.	3.8	1
4	One-step preparation of N-doped grapheme quantum dots with high quantum yield for bioimaging and highly sensitive electrochemical detection of isoniazid. , 2022, 135, 212731.		6
5	Review—Systematic Review on Electrochemical Biosensing of Breast Cancer miRNAs to Develop Alternative DCIS Diagnostic Tool. , 2022, 1, 021602.		39
6	Influence on effective and ineffective delamination of MXene (Ti3C2Tx) by tightly anchoring tin oxide nanocomposite for boosting the specific capacitance of supercapacitor. Journal of Alloys and Compounds, 2022, 921, 166092.	2.8	9
7	Magnetic nanoparticle-decorated graphene oxide-chitosan composite as an efficient nanocarrier for protein delivery. Colloids and Surfaces A: Physicochemical and Engineering Aspects, 2021, 610, 125913.	2.3	26
8	NiCo <sub>2</sub> O <sub>4</sub> nanoparticles inlaid on sulphur and nitrogen doped and co-doped rGO sheets as efficient electrocatalysts for the oxygen evolution and methanol oxidation reactions. Nanoscale Advances, 2021, 3, 3216-3231.	2.2	17
9	Enhanced electrochemical activities of morphologically tuned MnFe <sub>2</sub> O <sub>4</sub> nanoneedles and nanoparticles integrated on reduced graphene oxide for highly efficient supercapacitor electrodes. Nanoscale Advances, 2021, 3, 2887-2901.	2.2	30
10	Highly stable and selective LaNiO3nanostructures modified glassy carbon electrode for simultaneous electrochemical detection of neurotransmiting compounds. Colloids and Surfaces A: Physicochemical and Engineering Aspects, 2021, 618, 126387.	2.3	5
11	Rapid one-pot synthesis of PAM-GO-Ag nanocomposite hydrogel by gamma-ray irradiation for remediation of environment pollutants and pathogen inactivation. Chemosphere, 2021, 275, 130061.	4.2	26
12	Synergetic effect of hierarchical zinc oxide (ZnO) nanostructure with enhanced adsorption and antibacterial action towards waterborne detrimental contaminants. Applied Nanoscience (Switzerland), 2021, 11, 2181-2198.	1.6	1
13	ZnO-based electrochemical sensors for highly sensitive and selective detection of gallic acid at impact of substrate temperature. Applied Physics A: Materials Science and Processing, 2021, 127, 1.	1.1	1
14	Development of RF magnetron-sputtered molybdenum oxide-modified carbon cloth thin film as a ferulic acid sensor. Applied Physics A: Materials Science and Processing, 2021, 127, 1.	1.1	3
15	An electrochemical dopamine sensor based on RF magnetron sputtered TiO2/SS thin film electrode. Materials Letters, 2021, 300, 130175.	1.3	8
16	Enzyme like-colorimetric sensing of H2O2 based on intrinsic peroxidase mimic activity of WS2 nanosheets anchored reduced graphene oxide. Journal of Alloys and Compounds, 2021, 889, 161669.	2.8	26
17	Comparative Study of Biological (Phoenix loureiroi Fruit) and Chemical Synthesis of Chitosan-Encapsulated Zinc Oxide Nanoparticles and their Biological Properties. Arabian Journal for Science and Engineering, 2020, 45, 15-28.	1.7	8
18	Substrate temperature induced enhanced selectivity and sensitivity for nanomolar gallic acid detection on RF magnetron sputtered ZnO/GS thin film electrode. Sensors and Actuators A: Physical, 2020, 315, 112368.	2.0	7

#	Article	IF	CITATIONS
19	Engineering the surface of graphene oxide with bovine serum albumin for improved biocompatibility in <i>Caenorhabditis elegans</i> . Nanoscale Advances, 2020, 2, 5219-5230.	2.2	16
20	ZnO Nanorod Integrated Flexible Carbon Fibers for Sweat Cortisol Detection. ACS Applied Electronic Materials, 2020, 2, 499-509.	2.0	69
21	Fe2O3/polyaniline supramolecular nanocomposite: A receptor free sensor platform for the quantitative determination of serum creatinine. Analytica Chimica Acta, 2020, 1137, 103-114.	2.6	22
22	Effect of CuO, MoO3 and ZnO nanomaterial coated absorbers for clean water production. SN Applied Sciences, 2020, 2, 1.	1.5	8
23	Morphologically tuned LaMnO3 as an efficient nanocatalyst for the removal of organic dye from aqueous solution under sunlight. Journal of Environmental Chemical Engineering, 2020, 8, 104146.	3.3	22
24	A nanocomposite of NiFe <sub>2</sub> O <sub>4</sub> –PANI as a duo active electrocatalyst toward the sensitive colorimetric and electrochemical sensing of ascorbic acid. Nanoscale Advances, 2020, 2, 3481-3493.	2.2	28
25	Review—Towards Wearable Sensor Platforms for the Electrochemical Detection of Cortisol. Journal of the Electrochemical Society, 2020, 167, 067508.	1.3	53
26	Effect of cation substitution in MnCo2O4 spinel anchored over rGO for enhancing the electrocatalytic activity towards oxygen evolution reaction (OER). International Journal of Hydrogen Energy, 2020, 45, 6391-6403.	3.8	81
27	Tailoring the morphology and size of perovskite BiFeO3 nanostructures for enhanced magnetic and electrical properties. Materials and Design, 2020, 192, 108694.	3.3	46
28	Magnetic graphene/chitosan nanocomposite: A promising nano-adsorbent for the removal of 2-naphthol from aqueous solution and their kinetic studies. International Journal of Biological Macromolecules, 2020, 159, 530-538.	3.6	52
29	Mesoporous nickel oxide nanostructures: influences of crystalline defects and morphological features on mediator-free electrochemical monosaccharide sensor application. Nanotechnology, 2020, 31, 215501.	1.3	9
30	Nitrogen doped carbon nanofibers loaded with hierarchical vanadium tetrasulfide for the voltammetric detection of the non-steroidal anti-prostate cancer drug nilutamide. Mikrochimica Acta, 2019, 186, 141.	2.5	35
31	Surface Imprinted Ag Decorated MnO <sub>2</sub> Thin Film Electrodes for the Synergic Electrochemical Detection of Bacterial Pathogens. Journal of the Electrochemical Society, 2019, 166, G1-G9.	1.3	15
32	Carbon fiber based electrochemical sensor for sweat cortisol measurement. Scientific Reports, 2019, 9, 403.	1.6	105
33	MnCo <sub>2</sub> O <sub>4</sub> -rGO Hybrid Magnetic Nanocomposite Modified Glassy Carbon Electrode for Sensitive Detection of L-Tryptophan. Journal of the Electrochemical Society, 2019, 166, B845-B852.	1.3	31
34	Synthesis and Characterization of Hexagonal Prism like Zinc Oxide for Electrochemical Determination of Gallic Acid in Wine Samples. International Journal of Electrochemical Science, 2019, , 4769-4780.	0.5	7
35	<i>î±</i> -MoO <sub>3</sub> nanostructure on carbon cloth substrate for dopamine detection. Nanotechnology, 2019, 30, 265501.	1.3	21
36	Two dimensional α-MoO3 nanosheets decorated carbon cloth electrodes for high-performance supercapacitors. Colloids and Surfaces A: Physicochemical and Engineering Aspects, 2019, 569, 137-144.	2.3	49

#	Article	IF	CITATIONS
37	Design and fabrication of MEMS based intracranial pressure sensor for neurons study. Vacuum, 2019, 163, 204-209.	1.6	11
38	Self-Assembly of Nanostructured Hydroxyapatite Spheres for Photodegradation of Methylene Blue Dye. Materials Today: Proceedings, 2019, 18, 1729-1734.	0.9	8
39	Circumferential growth of zinc oxide nanostructure anchored over carbon fabric and its photocatalytic performance towards p-nitrophenol. Superlattices and Microstructures, 2019, 125, 159-167.	1.4	19
40	Effect of nano-coated CuO absorbers with PVA sponges in solar water desalting system. Applied Thermal Engineering, 2019, 148, 1416-1424.	3.0	66
41	Self-assembled SnO2/reduced graphene oxide nanocomposites via Langmuir-Blodgett technique as anode materials for Li-ion batteries. Materials Letters, 2018, 218, 295-298.	1.3	15
42	Surfactant-free solvothermal synthesis of Hydroxyapatite nested bundles for the effective photodegradation of cationic dyes. Journal of Physics and Chemistry of Solids, 2018, 116, 180-186.	1.9	15
43	Trace level electrochemical determination of the neurotransmitter dopamine in biological samples based on iron oxide nanoparticle decorated graphene sheets. Inorganic Chemistry Frontiers, 2018, 5, 705-718.	3.0	70
44	Facile synthesis of monodispersed 3D hierarchical Fe 3 O 4 nanostructures decorated r-GO as the negative electrodes for Li-ion batteries. Materials Research Bulletin, 2018, 97, 272-280.	2.7	20
45	Amine-functionalized diatom frustules: a platform for specific and sensitive detection of nitroaromatic explosive derivative. Environmental Science and Pollution Research, 2018, 25, 20540-20549.	2.7	9
46	Nanostructured SnO2 integrated conductive fabrics as binder-free electrode for neurotransmitter detection. Sensors and Actuators A: Physical, 2018, 269, 401-411.	2.0	22
47	N-Doped graphene with anchored ZnFe <sub>2</sub> O <sub>4</sub> nanostructures as an anode for lithium ion batteries with enhanced reversible capacity and cyclic performance. New Journal of Chemistry, 2018, 42, 16564-16570.	1.4	11
48	Highly selective and sensitive electrochemical detection of dopamine with hydrothermally prepared β-MnO2 nanostructures. Materials Science in Semiconductor Processing, 2018, 83, 216-223.	1.9	27
49	Detection of typhoid fever by diatom-based optical biosensor. Environmental Science and Pollution Research, 2018, 25, 20385-20390.	2.7	12
50	Tin Oxide/Reduced Graphene Oxide Nanocomposite-Modified Electrode for Selective and Sensitive Detection of Riboflavin. Journal of the Electrochemical Society, 2018, 165, B498-B507.	1.3	25
51	LaCoO <sub>3</sub> Nanostructures Modified Glassy Carbon Electrode for Simultaneous Electrochemical Detection of Dopamine, Ascorbic Acid and Uric Acid. Journal of the Electrochemical Society, 2017, 164, B152-B158.	1.3	26
52	Fabric Based Wearable Biosensor for Continuous Monitoring of Steroids. ECS Transactions, 2017, 77, 1841-1846.	0.3	11
53	N-doped Graphene/ZnFe2O4: A novel nanocomposite for intrinsic peroxidase based sensing of H2O2. Materials Research Bulletin, 2017, 95, 1-8.	2.7	39
54	Facile Approach for Synthesis of GO/ZnO Nanocomposite for Highly Efficient Photocatalytic Degradation of Organic Dyes under Visible Light. Nano Hybrids and Composites, 2017, 17, 121-126.	0.8	7

#	Article	IF	CITATIONS
55	Selective and low potential electrocatalytic oxidation and sensing of <scp>l</scp> -cysteine using metal impurity containing carbon black modified electrode. Analytical Methods, 2017, 9, 6791-6800.	1.3	20
56	Textile Fiber Electrode to Monitor Uric Acid as a Marker for Assessing Wound Chronicity. ECS Transactions, 2017, 80, 1277-1286.	0.3	2
57	Effect of Yb substitution on room temperature magnetic and dielectric properties of bismuth ferrite nanoparticles. Journal of Applied Physics, 2016, 120, .	1.1	16
58	Influence of supporting electrolytes on the structure of electrodeposited SnO2 thin films for energy storage applications. Ionics, 2016, 22, 1837-1846.	1.2	6
59	Electrochemical Simultaneous Detection of Dopamine, Ascorbic Acid and Uric Acid Using LaMnO <sub>3</sub> Nanostructures. Journal of the Electrochemical Society, 2016, 163, B460-B465.	1.3	26
60	Exchange spring magnetic behavior in BaFe12O19/Fe3O4 nanocomposites. Journal of Magnetism and Magnetic Materials, 2016, 406, 233-238.	1.0	44
61	Novel multiform morphologies of hydroxyapatite: Synthesis and growth mechanism. Applied Surface Science, 2016, 361, 25-32.	3.1	32
62	Influence of Growth Parameters on the Formation of Hydroxyapatite (HAp) Nanostructures and Their Cell Viability Studies. Nanobiomedicine, 2015, 2, 2.	4.4	46
63	Core–shell hydroxyapatite/Mg nanostructures: surfactant free facile synthesis, characterization and their in vitro cell viability studies against leukaemia cancer cells (K562). RSC Advances, 2015, 5, 48705-48711.	1.7	52
64	Hydrothermal synthesis of highly stable CuO nanostructures for efficient photocatalytic degradation of organic dyes. Materials Science in Semiconductor Processing, 2015, 30, 585-591.	1.9	95
65	Hydrothermal synthesis of novel Zn doped CuO nanoflowers as an efficient photodegradation material for textile dyes. Materials Letters, 2015, 144, 127-130.	1.3	56
66	Edge-carboxylated graphene anchoring magnetite-hydroxyapatite nanocomposite for an efficient 4-nitrophenol sensor. RSC Advances, 2015, 5, 13392-13401.	1.7	50
67	Superhydrophobic Ag decorated ZnO nanostructured thin film as effective surface enhanced Raman scattering substrates. Applied Surface Science, 2015, 355, 969-977.	3.1	31
68	Highly monodispersed Ag embedded SiO <sub>2</sub> nanostructured thin film for sensitive SERS substrate: growth, characterization and detection of dye molecules. RSC Advances, 2015, 5, 46229-46239.	1.7	21
69	Synthesis of hierarchical WO <sub>3</sub> nanostructured thin films with enhanced electrochromic performance for switchable smart windows. RSC Advances, 2015, 5, 96416-96427.	1.7	54
70	Electrodeposition of Macroporous SnO <sub>2</sub> Thin Films and Its Electrochemical Applications. Materials Focus, 2015, 4, 245-251.	0.4	3
71	Synthesis and Characterization of Mgo Nanoparticles by Neem Leaves through Green Method. Materials Today: Proceedings, 2015, 2, 4360-4368.	0.9	112
72	Improved microbial growth inhibition activity of bio-surfactant induced Ag–TiO2 core shell nanoparticles. Applied Surface Science, 2015, 327, 504-516.	3.1	14

#	Article	IF	CITATIONS
73	Enzymatic electrochemical glucose biosensors by mesoporous 1D hydroxyapatite-on-2D reduced graphene oxide. Journal of Materials Chemistry B, 2015, 3, 1360-1370.	2.9	148
74	Formulation Of SnO2/graphene Nanocomposite Modified Electrode For Synergitic Electrochemcial Detection Of Dopamine. Advanced Materials Letters, 2015, 6, 973-977.	0.3	14
75	Hydrophilic polymer coated monodispersed Fe <sub>3</sub> O <sub>4</sub> nanostructures and their cytotoxicity. Materials Research Express, 2014, 1, 015015.	0.8	19
76	Electrochemical performance of SnO2 hexagonal nanoplates. Ionics, 2014, 20, 335-346.	1.2	7
77	An in vitro analysis of H1N1 viral inhibition using polymer coated superparamagnetic Fe3O4 nanoparticles. RSC Advances, 2014, 4, 13409.	1.7	37
78	Quercetin conjugated superparamagnetic magnetite nanoparticles for in-vitro analysis of breast cancer cell lines for chemotherapy applications. Journal of Colloid and Interface Science, 2014, 436, 234-242.	5.0	102
79	Facile in situ growth of Fe <sub>3</sub> O <sub>4</sub> nanoparticles on hydroxyapatite nanorods for pH dependent adsorption and controlled release of proteins. RSC Advances, 2014, 4, 50510-50520.	1.7	34
80	Shape evolution and size controlled synthesis of mesoporous hydroxyapatite nanostructures and their morphology dependent Pb( <scp>ii</scp> ) removal from waste water. RSC Advances, 2014, 4, 37446-37457.	1.7	54
81	Effect of NaOH concentration on structural, surface and antibacterial activity of CuO nanorods synthesized by direct sonochemical method. Superlattices and Microstructures, 2014, 66, 1-9.	1.4	57
82	Diatom-Based Label-Free Optical Biosensor for Biomolecules. Applied Biochemistry and Biotechnology, 2014, 174, 1166-1173.	1.4	33
83	Electrochemical behavior of nanostructured SnO2 thin films in aqueous electrolyte solutions. Materials Science in Semiconductor Processing, 2014, 26, 55-61.	1.9	17
84	Rheological behavior and electrical properties of polypyrrole/thermally reduced graphene oxide nanocomposite. Colloids and Surfaces A: Physicochemical and Engineering Aspects, 2014, 441, 614-622.	2.3	37
85	Rheological behavior ―Electrical and thermal properties of polypyrrole/graphene oxide nanocomposites. Journal of Applied Polymer Science, 2014, 131, .	1.3	20
86	Effect Of Catalyst Concentration On The Synthesis Of MWCNT By Single Step Pyrolysis. Advanced Materials Letters, 2014, 5, 543-548.	0.3	4
87	Surfactant free solvothermal synthesis of monodispersed 3D hierarchical Fe3O4 microspheres. Materials Letters, 2013, 110, 98-101.	1.3	15
88	Conducting polyaniline-graphene oxide fibrous nanocomposites: preparation, characterization and simultaneous electrochemical detection of ascorbic acid, dopamine and uric acid. RSC Advances, 2013, 3, 14428.	1.7	130
89	Influence of growth and photocatalytic properties of copper selenide (CuSe) nanoparticles using reflux condensation method. Applied Surface Science, 2013, 283, 802-807.	3.1	47
90	Optical and electrochemical studies of polyaniline/SnO2 fibrous nanocomposites. Materials Research Bulletin, 2013, 48, 640-645.	2.7	46

#	Article	IF	CITATIONS
91	Novel Synthesis of LaFeO <sub>3</sub> Nanostructure Dendrites: A Systematic Investigation of Growth Mechanism, Properties, and Biosensing for Highly Selective Determination of Neurotransmitter Compounds. Crystal Growth and Design, 2013, 13, 291-302.	1.4	115
92	Shape evolution of perovskite LaFeO3 nanostructures: a systematic investigation of growth mechanism, properties and morphology dependent photocatalytic activities. RSC Advances, 2013, 3, 7549.	1.7	206
93	Enhanced photocatalytic performance of novel self-assembled floral β-Ga2O3 nanorods. Current Applied Physics, 2013, 13, 652-658.	1.1	41
94	Effect of annealing and electrochemical properties of sol–gel dip coated nanocrystalline V2O5 thin films. Materials Science in Semiconductor Processing, 2013, 16, 256-262.	1.9	53
95	Organic additives assisted synthesis of mesoporous β-Ga <sub>2</sub> O <sub>3</sub> nanostructures for photocatalytic dye degradation. Semiconductor Science and Technology, 2013, 28, 035015.	1.0	29
96	Synthesis, morphology, optical and photocatalytic performance of nanostructured β-Ga2O3. Materials Research Bulletin, 2013, 48, 2296-2303.	2.7	44
97	Graphene nanosheets by low-temperature thermal reduction of graphene oxide using RF-CVD. Journal of Experimental Nanoscience, 2013, 8, 311-319.	1.3	9
98	Electrodeposition of Sno[sub 2] nanoneedles on anodized copper substrates and its electrochemical performance. , 2013, , .		2
99	A comparative analysis of green synthesis approach starch capped metal oxides (ZnO & CdO) nanoparticles and its bacterial activity. , 2013, , .		2
100	Electrodeposition of V2O5 nanorods on current collector substrate. , 2012, , .		0
101	Controlled synthesis of perovskite LaFeO3 microsphere composed of nanoparticles via self-assembly process and their associated photocatalytic activity. Chemical Engineering Journal, 2012, 209, 420-428.	6.6	172
102	Novel synthesis of silver nanoparticles using 2,3,5,6-tetrakis-(morpholinomethyl) hydroquinone as reducing agent. Spectrochimica Acta - Part A: Molecular and Biomolecular Spectroscopy, 2012, 95, 305-309.	2.0	8
103	Strong quantum confinement effect in nanocrystalline cerium oxide. Materials Letters, 2011, 65, 2635-2638.	1.3	51
104	Self assembly of Co doped CeO2 microspheres from nanocubes by hydrothermal method and their photodegradation activity on AO7. Materials Letters, 2011, 65, 3320-3322.	1.3	26
105	Preparation of New Reducing Agent for the Synthesis of Silver Nanoparticles. , 2011, , .		2
106	Molecular nanodevices based on functionalized cyclodextrins. Physica Status Solidi (A) Applications and Materials Science, 2008, 205, 2532-2535.	0.8	2
107	Sheathing Polymer Gels Fibrils with Nanotubules. Macromolecular Symposia, 2007, 251, 11-14.	0.4	0
108	Electrical conductivity and single oscillator model properties of amorphous CuSe semiconductor thin film. Journal of Non-Crystalline Solids, 2007, 353, 2934-2937.	1.5	38

#	Article	IF	CITATIONS
109	The effect of annealing on vacuum-evaporated copper selenide and indium telluride thin films. Materials Characterization, 2007, 58, 756-764.	1.9	47
110	Preparation and characterization of electrodeposited indium selenide thin films. Crystal Research and Technology, 2005, 40, 557-562.	0.6	45
111	Influence of substrate temperature on the properties of vacuum evaporated InSb films. Crystal Research and Technology, 2005, 40, 573-578.	0.6	36
112	Effect of substrate temperature on the properties of vacuum evaporated indium selenide thin films. Crystal Research and Technology, 2005, 40, 658-664.	0.6	9
113	Space charge limited current, variable range hopping and mobility gap in thermally evaporated amorphous InSe thin films. Journal of Materials Science: Materials in Electronics, 2004, 15, 787-792.	1.1	16
114	Conduction studies on electrodeposited indium selenide thin films. Ionics, 2004, 10, 300-303.	1.2	9
115	Characterization of vacuum evaporated In - Se thin films. Ionics, 2004, 10, 311-316.	1.2	7
116	<title>Characterization of vacuum-evaporated&lt;br&gt;In&lt;formula&gt;&lt;inf&gt;&lt;roman&gt;70&lt;/roman&gt;&lt;/inf&gt;&lt;/formula&gt;Se&lt;formula&gt;&lt;inf&gt;&lt;roman&gt;30&lt;/roman&gt;&lt;/inf&gt;&lt;/formula&gt;&lt;br&gt;thin films</title> . , 2004, 5774, 283.		0
117	Optical constants of DC magnetron sputtered titanium dioxide thin films measured by spectroscopic ellipsometry. Crystal Research and Technology, 2003, 38, 773-778.	0.6	49
118	Sm3+ rare-earth doping in non-noble metal oxide –WO3 grown on carbon cloth fibre as a bifunctional electrocatalyst for high-performance water electrolysis. Sustainable Energy and Fuels, 0, , .	2.5	7
119	Revealing the Role of BrĄ̃nsted Basicity by the Electrocatalytic Reaction via Li Insertion in the MgFe <sub>2</sub> O <sub>4</sub> Lattice. Journal of Physical Chemistry C, 0, , .	1.5	1